

**Investigation of modal damage-sensitive features of a scaled three-storey steel frame for vibration-based damage detection.**

Marafini, Francesca; Zini, Giacomo; Barontini, Alberto; Monchetti, Silvia; Betti, Michele; Bartoli, Gianni; Mendes, Nuno; Cicirello, Alice

**DOI**

[10.1088/1742-6596/2647/18/182043](https://doi.org/10.1088/1742-6596/2647/18/182043)

**Publication date**

2024

**Document Version**

Final published version

**Published in**

Journal of Physics: Conference Series

**Citation (APA)**

Marafini, F., Zini, G., Barontini, A., Monchetti, S., Betti, M., Bartoli, G., Mendes, N., & Cicirello, A. (2024). Investigation of modal damage-sensitive features of a scaled three-storey steel frame for vibration-based damage detection. *Journal of Physics: Conference Series*, 2647(18), Article 182043. <https://doi.org/10.1088/1742-6596/2647/18/182043>

**Important note**

To cite this publication, please use the final published version (if applicable).  
Please check the document version above.

**Copyright**

Other than for strictly personal use, it is not permitted to download, forward or distribute the text or part of it, without the consent of the author(s) and/or copyright holder(s), unless the work is under an open content license such as Creative Commons.

**Takedown policy**

Please contact us and provide details if you believe this document breaches copyrights.  
We will remove access to the work immediately and investigate your claim.

PAPER • OPEN ACCESS

## Investigation of modal damage-sensitive features of a scaled three-storey steel frame for vibration-based damage detection.

To cite this article: Francesca Marafini *et al* 2024 *J. Phys.: Conf. Ser.* **2647** 182043

View the [article online](#) for updates and enhancements.

### You may also like

- [Estimation of bolt tension using transverse natural frequencies of the shank and protruding end](#)  
D. S. Rashid, F. Giorgio-Serchi, N. Hosoya et al.
- [Vibration-based FE-model updating for strain history estimation of a 3MW offshore wind turbine tower](#)  
Sandro D R Amador, Søren Rasmussen, Rune Brincker et al.
- [Vibration-based system identification of a large steel box girder bridge](#)  
R Schneider, P Simon, F Hille et al.



**PRIME<sup>TM</sup>**  
PACIFIC RIM MEETING  
ON ELECTROCHEMICAL  
AND SOLID STATE SCIENCE  
**HONOLULU, HI**  
October 6-11, 2024

*Joint International Meeting of*  
The Electrochemical Society of Japan (ECSJ)  
The Korean Electrochemical Society (KECS)  
The Electrochemical Society (ECS)

Early Registration Deadline:  
**September 3, 2024**

**MAKE YOUR PLANS  
NOW!**

# Investigation of modal damage-sensitive features of a scaled three-storey steel frame for vibration-based damage detection.

**Francesca Marafini<sup>1</sup>, Giacomo Zini<sup>1</sup>, Alberto Barontini<sup>2</sup>, Silvia Monchetti<sup>1</sup>, Michele Betti<sup>1</sup>, Gianni Bartoli<sup>1</sup>, Nuno Mendes<sup>2</sup>, Alice Cicirello<sup>3</sup>.**

<sup>1</sup> Department of Civil and Environmental Engineering (DICEA), University of Florence, Florence, Italy

<sup>2</sup> University of Minho, ISISE, ARISE, Department of Civil Engineering, Guimarães, Portugal

<sup>3</sup> Faculty of Civil Engineering and Geosciences, Department of Engineering Structures, Section of Mechanics and Physics of Structures (MPS), Delft University of Technology, Stevinweg 1, Delft 2628, Netherlands

francesca.marafini@unifi.it

**Abstract.** The application of vibration-based Structural Health Monitoring (SHM) for damage detection is characterised by three fundamental aspects: the features extracted as representative of the structural condition that can be directly linked to some form of damage, the metrics selected as novelty or damage index, and the statistical model or classifier built to identify underlying patterns indicative of changes in the structure's state. Focusing on the first step to improve the performance of vibration-based SHM strategies, the extracted features should be robust to noise, sensitive to the presence of a specific type of damage. Further, damage should induce patterns that are distinguishable from environmental and operational variabilities and other forms of damage such as ageing phenomena. In this paper, the problem is framed as an outlier detection problem and the use of different modal parameters as Damage Sensitive Features (DSFs) is investigated, evaluating them based on the detection performance of an unsupervised One-Class Support Vector Machine (OCSVM) classifier. In particular, an artificial dataset is generated from the calibrated numerical model of a three-storey steel frame structure in different damage scenarios. The methodology is validated against available experimental data. For the case investigated the natural frequencies were sensitive to damage and robust to noise.

## 1. Introduction

Ensuring the safety and reliability of engineering structures and effectively managing their maintenance are critical factors that have made Structural Health Monitoring (SHM) techniques indispensable. SHM provides a framework that is based on the continuous tracking of structural response, aiming at evaluating damage (i.e. detecting, localizing, quantifying its extent, and predicting the remaining useful life of the structure) [1]. Within this hierarchy, detection is, thus, the first task to address, vibration-based SHM techniques have now an established role in this framework due to their non-invasive nature and ability to provide insights on the global behaviour in almost real-time [2]. To this end, Damage-Sensitive Features (DSFs) are extracted from the measured vibration signals and compared against a



healthy reference state in a Statistical Pattern Recognition (SPR) framework [3]. If an a-priori knowledge of the damaged behaviour is missing, this process is referred to as outlier detection, which can be addressed through unsupervised Machine-Learning (ML) inference [5].

The effectiveness of these approaches depends largely on: (i) the selection of appropriate DSFs [4], (ii) the use of appropriate metrics as damage indices, and (iii) the choice of algorithm architecture to identify patterns indicating the presence of damage [5]. This paper is mainly concerned with the first aspect, thus, the sensitivity of different modal parameters to damage is compared, presenting the preliminary results of a vibration-based damage identification methodology, based on an unsupervised classification strategy that requires a limited number of parameters for model setup: the One-Class Support Vector Machine (OCSVM). A case study of a three-storey steel frame structure is used as reference to evaluate the sensitivity of the chosen DSFs to localized damage, and their robustness to noise and environmental variabilities. Both experimental data and numerical simulations are used in this investigation to test the detection performance of the outlier detection algorithm investigated.

## 2. Methodology

A case-study is developed to validate and test a damage identification strategy and each feature sensitivity to damage. This is a scaled three-storey steel frame tested in an outdoor environment at the University of Florence. The frame was subjected to Ambient Vibration Testing (AVTs), in the undamaged state (UD) and under eleven scenarios of increasing damage (D#) (see Section 3). Natural frequencies and mode shapes were assessed in all these scenarios with the Automatic Operational Modal Analysis (A-OMA) procedure described in [6] using a Stochastic Subspace Identification (SSI) technique. To test the damage identification strategy, a large artificial dataset was generated through a numerical model developed in DIANA FEA [7], which was calibrated to the undamaged condition. This model has a twofold purpose, as it allows the simulation of selected experimental damage scenarios as well as the effect of environmental and operational variations (EOVs) on the modal properties. The artificial dataset was generated, by operating sequential eigenvalue analyses, under changing environmental conditions with reference to the linear relationship between the steel Young's Modulus and temperature variation available in [8].

Frequencies and mode shapes were chosen at this stage as the DSFs for comparison, and reference undamaged features were defined. The root-mean-square error in terms of frequency (RMSE) and the Modal Assurance Criterion value (MAC) and the Coordinate Assurance Criterion (COMAC) value were selected as damage indices. Outlier detection was operated by training an unsupervised One-Class Support Vector Machine (OCSVM) [9] algorithm on the numerical dataset, and by testing it on both numerical and experimental A flowchart of the adopted methodology is shown in Figure 1 and the main steps are discussed in the following sections.

## 3. The benchmark structure

The analysed structure is a three-storey steel frame with fully welded H-columns and I-beams (Figure 2a) and additional flanges in the connections. The slabs are made of six concrete blocks supported by two UPN embedded profiles, welded on the beams of the frame. The ground level consists of a ribbed steel sheet, welded to the perimeter beams with a 5 cm overhang.

The structure was instrumented with twelve uniaxial piezoelectric accelerometers (10 V/g sensitivity, 0.1-1500 Hz range) positioned at all levels at two opposite corners, in both directions, as shown in Figure 2b-e. Damage was progressively imposed on the structure by cutting the flanges of the columns in four sections (S1 to S4), for a total of eleven damage scenarios (Figure 2c,d). A summary of the structure characteristics and damage scenarios is provided in Table 1.

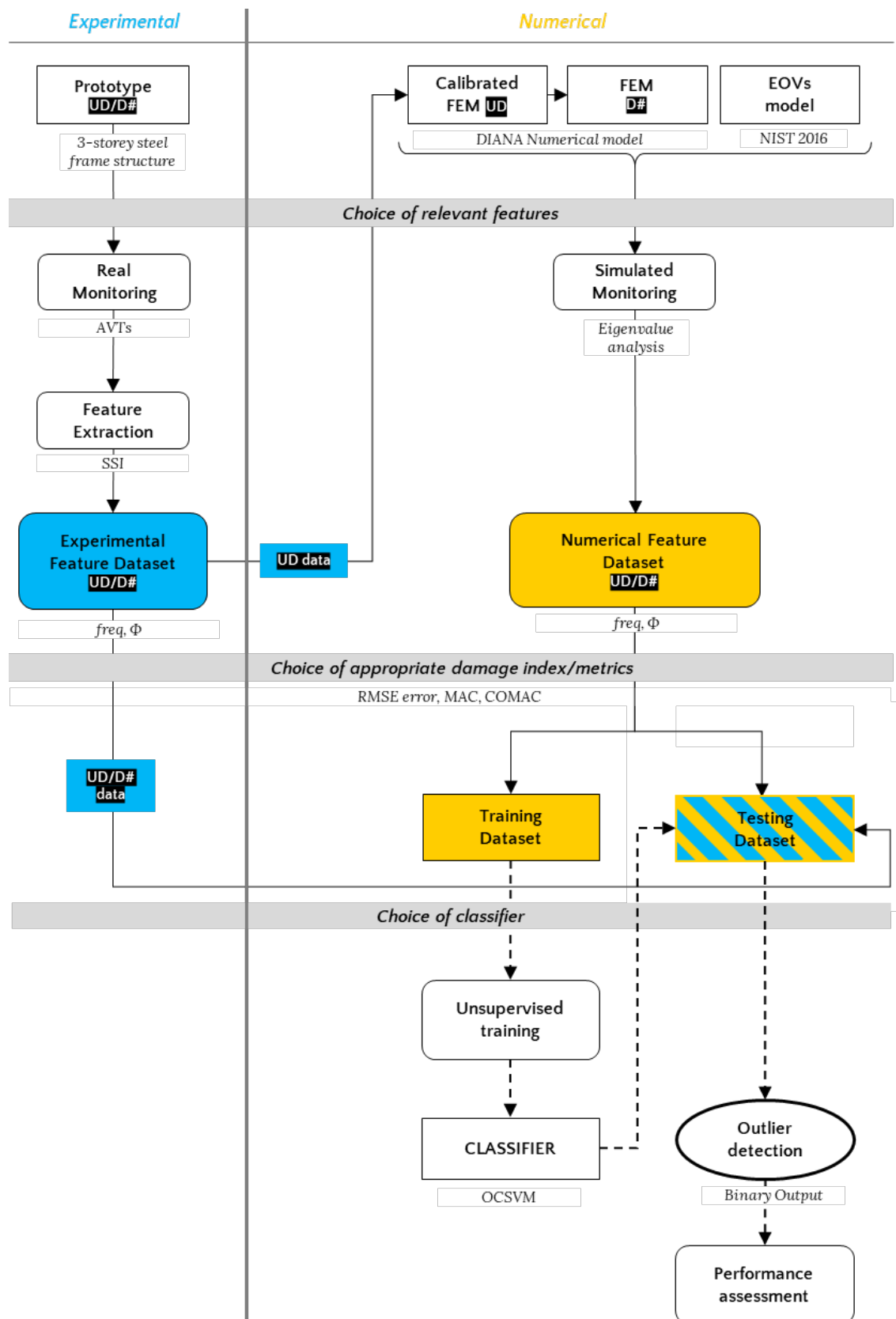


**Figure 1.** Workflow of the proposed methodology. The dotted line represents the unsupervised outlier detection phase. In *italics*, the specific choices operated in the present work.



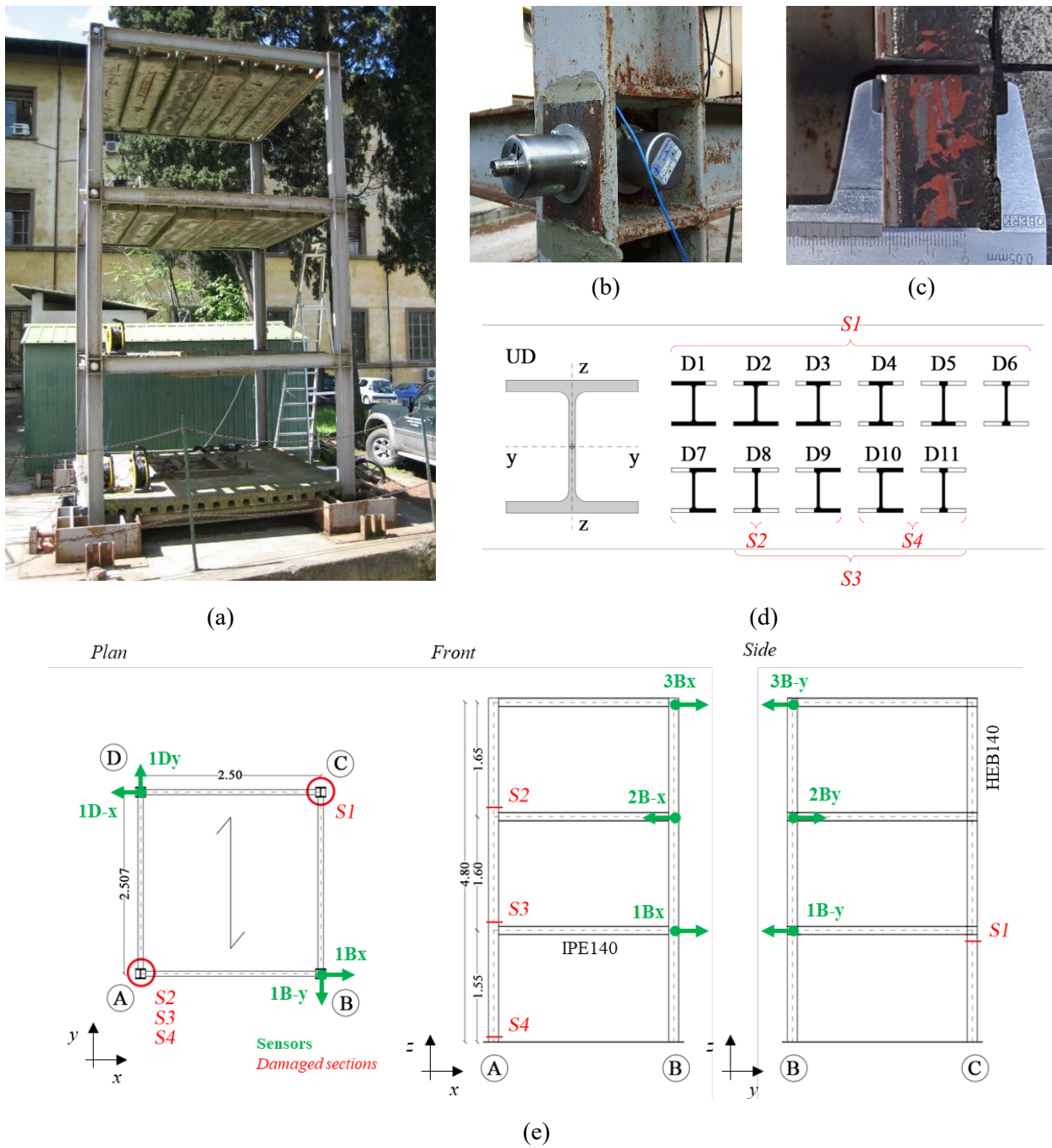


**Figure 2.** (a) Benchmark structure, (b) piezoelectric accelerometers, (c) imposed cut to the flange, (d) damage scenarios, (e) instrumented locations for dynamic identification with tags and orientation with respect to the reference systems (sensors in green; damaged sections in red; dimensions in meters).

**Table 1.** Material properties and % ranges of decrease of damaged section properties (area and inertia).

Material properties			Section	Damage scenario	$\Delta_{Area}$ [%]	$\Delta_{J_{xx}}$ [%]	$\Delta_{J_{yy}}$ [%]
$E_{steel}$	206	[GPa]	S1	#DS1 - #DS6	9-66	12-77	23-99
$\delta_{steel}$	30	[GPa]	S2	#DS7	33.5	40	50
$E_{concrete}$	7850	[kg/m <sup>2</sup> ]	S2-S3	#DS8 - #DS9	32-64	37-75	50-99
$\delta_{slab}$	22	[kN]	S3-S4	#DS10 - #DS11	32-64	37-75	50-99

#### 4. Experimental results

The AVTs were conducted in seven non-consecutive days. Each acquisition was 30 minutes long, with a sampling rate of 600 Hz. The signals were filtered between 0.3 and 30 Hz and resampled at 60 Hz, and the RMS was calculated for each instrument in each test to understand the vibration intensity. A-OMA was operated excluding a few signals identified as sources of noise in the frequency band from 0 to 16 Hz, leading to sharper spectral densities.

Acceleration signals from all acquisitions were processed to obtain the natural frequencies and mode shapes of the structure across all damage scenarios. Seven natural frequencies were identified (see Figure 3) across all damage scenarios with a high level of certainty, namely the first three bending modes in  $x$ -direction, the first two bending in  $y$ -direction and two torsional modes. Their evolution in time is shown in Figure 3, together with specification of the occurrence of each damage scenario. The results of the twelve sensors installed were not sufficient for the representation of the torsional mode shapes. Therefore, the following analysis is limited to 5 bending mode shapes.

From an initial analysis of the experimental data, the bending mode shapes in the  $x$ -direction showed to be affected by damage more than the ones in the  $y$ -direction, consistently with the higher percentage decrease of inertia  $J_{yy}$  in the following scenarios (see Table 1). This is evident when normalised frequency values are compared for the distinct damage scenarios (see Figure 3).

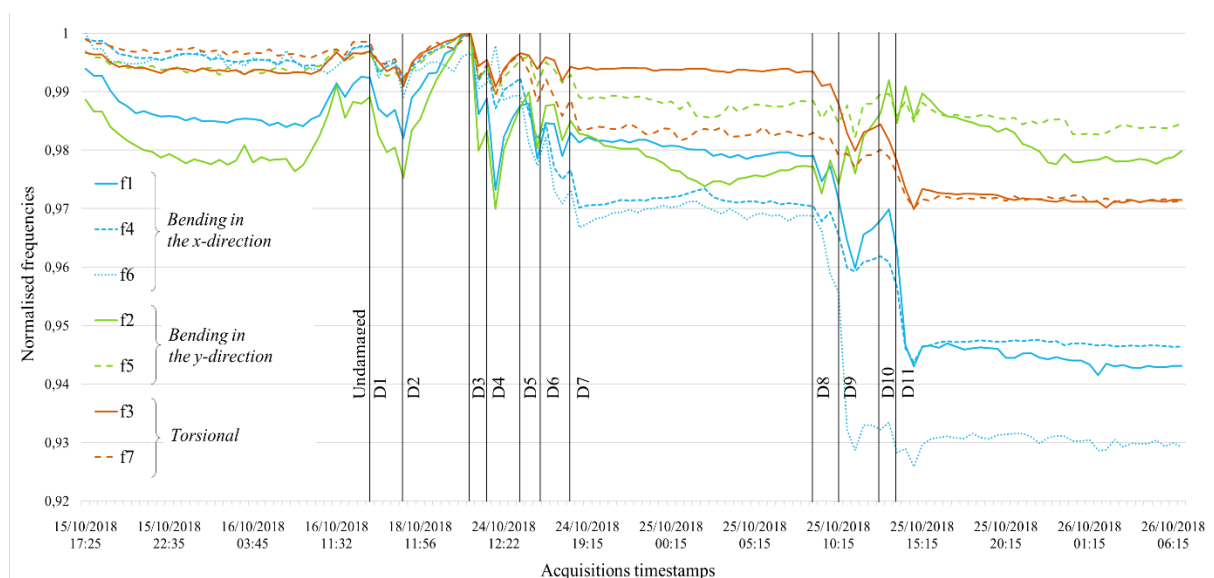


**Figure 3.** Experimental frequencies for all acquisitions, with specification of the occurrence of each damaged scenarios imposed on the structure.

#### 5. Numerical modelling and calibration

A numerical model was developed in DIANA FEA based on the linear material properties in Table 1 and calibrated on the experimental results for the UD state. Flat shell elements (CQ40F) were chosen to model the steel profile, to allow for the simulation of the localized damage imposed in the experimental tests. The final model was obtained by applying a rotational spring in the  $x$ -direction at the base, providing calibration errors lower than 1% for the 1<sup>st</sup> and 2<sup>nd</sup> frequencies. Subsequently, damage scenarios D6 and D11 were simulated in the numerical model. These scenarios were selected as both providing significant damage to the sections, but with very different extent at the global level. The torsional modes were not selected as DSFs, given the higher calibration error and the lack of complete representation of the experimental mode shapes for comparison with the undamaged state. The results of the calibration are shown both in Figure 4 and Table 2.

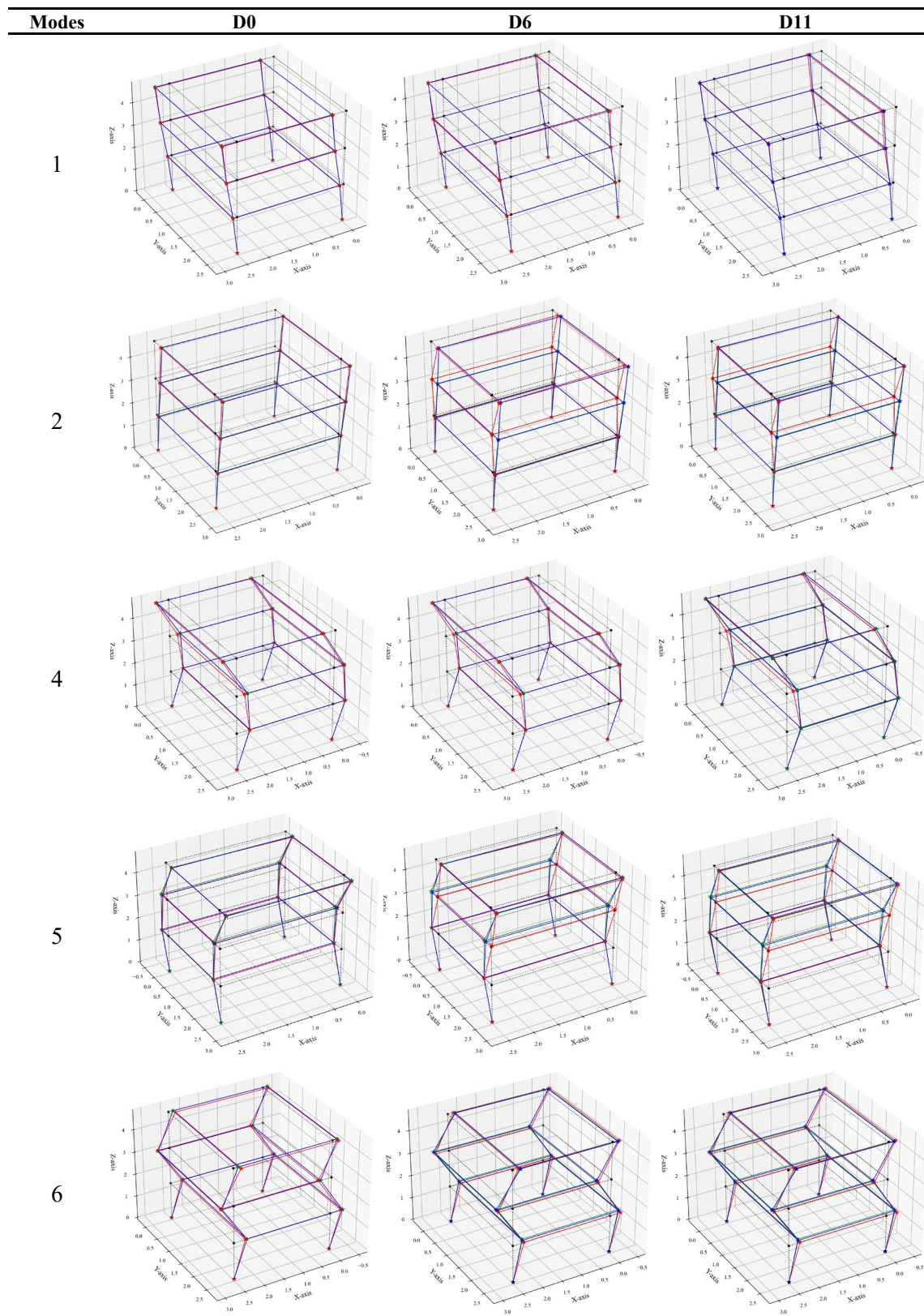


**Figure 4.** Results of the numerical model calibrations. Comparison of bending mode shapes for experimental (in red) and numerical (in blue) data.



**Table 2.** Calibration results in terms of frequencies, calibration error  $\varepsilon$  and frequencies variations both numerical and experimental, highlighted in green calibration errors below 3.5%.

Modes	UD				D6						D11					
	$f_{exp}$	$f_{num}$	$\varepsilon$	MAC	$f_{exp}$	$f_{num}$	$\varepsilon$	MAC	D <sub>D6,exp</sub>	D <sub>D6,num</sub>	$f_{exp}$	$f_{num}$	$\varepsilon$	MAC	D <sub>D11,exp</sub>	D <sub>D11,num</sub>
1	3.098	3.083	0.5%	0.996	3.077	3.077	0.0%	0.992	-0.70%	-0.21%	2.942	2.880	2.1%	0.990	-5.04%	-6.58%
2	3.760	3.742	0.5%	0.994	3.748	3.741	0.2%	0.793	-0.33%	-0.02%	3.712	3.695	0.5%	0.825	-1.28%	-1.26%
3	6.271	6.001	4.3%	0.997	6.263	5.990	4.4%	0.860	-0.13%	-0.18%	6.111	5.816	4.8%	0.982	-2.56%	-3.08%
4	10.019	10.330	3.1%	0.979	9.821	10.108	2.9%	0.965	-1.97%	-2.15%	9.516	9.227	3.0%	0.963	-5.02%	-10.68%
5	13.733	13.815	0.6%	0.987	13.686	13.729	0.3%	0.820	-0.34%	-0.62%	13.532	13.435	0.7%	0.794	-1.46%	-2.75%
6	16.094	17.633	9.6%	0.957	15.751	17.034	8.1%	0.940	-2.13%	-3.40%	15.031	15.388	2.4%	0.957	-6.60%	-12.73%
7	21.585	21.111	2.2%	0.974	21.407	20.875	2.5%	0.936	-0.83%	-1.12%	21.025	20.708	1.5%	0.861	-2.59%	-1.91%

## 6. Simulated monitoring under varying temperature conditions

The model in the three analysed scenarios (UD, D6 and D11) was used to generate synthetic data with the objective of generating a larger volume of data with respect to the experimental acquisition, and build a training and testing dataset for the OCSVM classifier. Sequential eigenvalue analysis was operated, assuming hourly acquisitions over the course of three years, one year for each scenario. The value of the  $E_{steel}$  was changed at each simulated acquisition as per (1), in which  $E_0$  is the value of  $E$  at 20°C (see Table 1),  $T^*$  the temperature and  $e_1$ ,  $e_2$ ,  $e_3$ , and  $e_4$  a set of constants obtained experimentally in [8].

$$E(T) = E_0 \exp \left( -\frac{1}{2} \left( \frac{T^*}{e_3} \right)^{e_1} - \frac{1}{2} \left( \frac{T^*}{e_4} \right)^{e_2} \right) \quad (1)$$

Temperature data was obtained for three consecutive years from a meteorological station in the vicinity of the real specimen [10]. The data obtained showed both the presence of seasonality and visible damage effects, as shown in Figure 5. From each eigenvalue analysis, both frequencies and mode shapes were extracted. Finally, to simulate the natural variability of real-world data, a random Gaussian noise with zero mean and 0.01 standard deviation was added to the features time series.

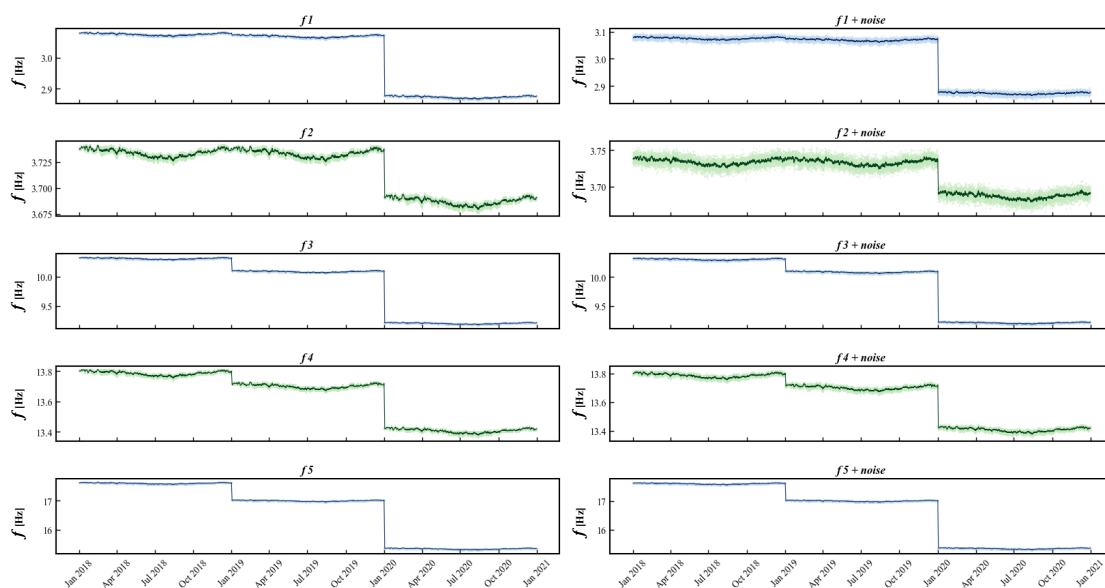


**Figure 5.** Artificial frequencies before (left) and after (right) the addition of noise, over the three years of simulated monitoring (the bending modes in the  $x$ -direction are in blue, in the  $y$ -direction in green).

## 7. Outlier detection

Once the simulated monitoring was available, damage indices were calculated from the selected DSFs. The temperature, the frequency RMSE, the MAC and the COMAC values calculated with respect to the first simulated acquisition, were combined in different feature matrices to operate the comparison (see Table 3). All data was normalized with 0 mean and unit standard deviation before training. The purpose of the outlier detection was to conduct a simple binary classification: undamaged (UD) and damaged (without distinction between scenarios D6 and D11). A first set of OCSVM models were fitted to 9 months of undamaged numerical samples and tested on the remaining numerical data. These classifiers were trained setting the minimum possible value of contamination, without adjusting the default hyperparameters in this first instance, apart from the value of  $\nu$  (the fraction of training data that is allowed to be classified as outliers), which was set according to the chosen contamination. The choice of contamination rate of the training set was done under the assumption that a training set without damage data is the condition closer to a real-world application.

**Table 3.** Different feature matrices defined for the comparison.

Classifiers	DSFs	N. of DSFs
1	T, RMSE <sub>f</sub> , MAC, COMAC	23
2	RMSE <sub>f</sub>	5
3	T, RMSE <sub>f</sub>	6
4	RMSE <sub>f</sub> , MAC	10
5	T, RMSE <sub>f</sub> , MAC	11
6	MAC	5
7	COMAC	12
8	MAC, COMAC	17
9	RMSE <sub>f</sub> , MAC, COMAC	22

The performance of each model was evaluated by compiling a confusion matrix, which includes the four outputs of binary classification: True Positives (TP), False Positives (FP), True Negatives (TN) and False Negatives (FN). In Table 4 the following performance metrics are reported: the *recall* (TP rate), the *probability of false alarms* (FP rate), the *specificity* (TN rate), the *type II error rate* (FN rate) and the *f1 score* metric, the latter accounting for the unbalanced class distribution [11]. The results of this first classification for all nine classifiers are shown in Table 4.

The performance evaluation results showed how the classifiers 6 to 8, which only used MAC and COMAC values as features, did not yield an adequate classification output. Meanwhile, all others appeared to be equivalent, with classifiers 1 and 9 showing the highest recall. Classifier 9 was selected to be tested on an additional testing dataset, composed of twelve experimental acquisitions, one for each damage scenario, but no outliers were identified. This tolerant behaviour of the classifier may be due to the overfitting to training data and in general to the unbalanced distribution of classes in the training set, missing damaged samples. Therefore, all the models were re-run with a contamination of 10% of the training dataset (sourced from the D6 scenario), yielding results more heterogeneous than before. Classifier 2 showed the best classification performance both in the training (finding 85% of the outliers in the training) and in the testing datasets. The predictions for the contaminated training dataset are plotted in Figure 6, showing correct results not only in terms of overall percentage but also in terms of specificity. Classifier 2 with 10% contamination was then tested again on the experimental dataset, predicting outliers for the last 5 damage scenarios involving multiple damaged sections, from D7 to D11 (see Figure 7).

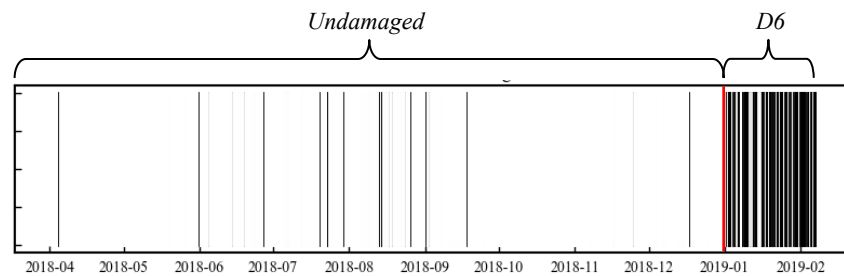


**Figure 6.** Classification results for classifier 2 with contamination of 10% on the training dataset.

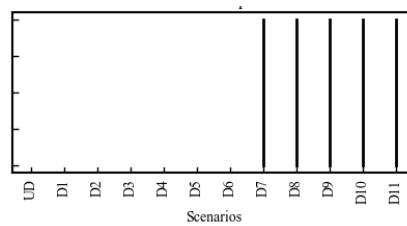


**Figure 7.** Classification results for classifier 2 with contamination of 10% on the experimental dataset.

**Table 4.** Performance metrics for all OCSVM models, with both minimum and 10% contamination. In red are highlighted the worst performing models and in green the two top classifiers.

Contamination 0.1%				Contamination 10%					
Classifier	Testing			Training		Testing			F1 score
	TP rate	FP rate	F1 score	TP rate	FP rate	TP rate	FP rate		
	TN rate	FP rate		TN rate	FP rate	TN rate	FP rate		
1	99.99% 100 %	0.00% 0.01%	1,00	23,86% 91,84%	8,15% 76,14%	73,59% 92,33%	7,67% 26,41%	0,84	
2	99.77% 100 %	0.00% 0.23%	1,00	71,58% 98,20%	1,80% 28,42%	94,81% 98,26%	1,74% 5,19%	0,97	
3	99.79% 100 %	0.00% 0.21%	1,00	59,13% 96,54%	3,46% 40,87%	93,39% 94,20%	5,80% 6,61%	0,96	
4	99.76% 100 %	0.00% 0.24%	1,00	54,11% 95,88%	4,12% 45,89%	89,29% 95,98%	4,02% 10,71%	0,94	
5	99.78% 100 %	0.00% 0.22%	1,00	46,46% 94,86%	5,14% 53,54%	88,67% 93,79%	6,21% 11,33%	0,94	
6	0.15% 99.77 %	0.23% 99.91%	0,00	9,25% 89,89%	10,11% 90,75%	10,29% 91,19%	8,81% 89,71%	0,19	
7	0.09% 99.86 %	0.14% 99.77%	0,00	9,70% 89,95%	10,05% 90,30%	9,75% 91,05%	8,95% 90,25%	0,18	
8	0.11% 99.77 %	0.23% 99.89%	0,00	9,70% 89,95%	10,05% 90,30%	10,09% 90,23%	9,77% 89,91%	0,18	
9	99.99% 100 %	0.00% 0.01%	1,00	24,09% 91,87%	8,13% 75,91%	73,29% 92,47%	7,53% 26,71%	0,84	

## 8. Conclusions

This paper has investigated the development of a case study to assess the robustness of certain DSFs to other phenomena such as temperature variability and noise. To this end, a classifier was trained on numerical data, and then tested on experimental data, allowing a 10% contamination of the training dataset with numerical outliers. The performance evaluation indicated that, under the provided assumptions and methodology limitations, the natural frequencies were sensitive to damage, regardless of their use in combination with other features. The lower levels of damage were not detected from the experimental dataset, but the classifier trained on the frequency RMSE could detect the most severe damage scenarios once its training was contaminated with a 10% of synthetic outliers.

There are several limitations that need to be considered. The simulation of EOVs was limited to the inversely proportional relationship between temperature and material stiffness, neglecting other phenomena that could potentially affect the vibration dataset and undermine the soundness of the numerical dataset. Despite the limitations, this research contributes to a deeper understanding of the use of vibration data for damage detection, and opens the way to advance the proposed methodology further.

Further study will focus on the effectiveness of the classifiers without contamination, by removing the effect of applied EOVs, as well as by varying the threshold defined by the OCSVM. Hyperparameters setting will be explored to improve the methodology. Additionally, other feature space options will be analysed to provide further insights into their distinct sensitivity to damage, for example by analysing the x and y-direction separately. Finally, extending the scope of this research, the developed numerical model will be used to explore the effects on the vibration-based DSFs of damage due to ageing and of other environmental and operating variabilities.

## 9. References

1. Rytter A, (1993) Vibrational Based Inspection of Civil Engineering Structures. Fracture and Dynamics Vol. R9314 No. 44, Aalborg University
2. Farrar CR, Doebling SW, Nix DA (2001) Vibration-based structural damage identification. Philosophical Transactions of the Royal Society A: Mathematical, Physical and Engineering Sciences 359:131–149
3. Farrar CR, Worden K (2012) Structural Health Monitoring: A Machine Learning Perspective. Structural Health Monitoring: A Machine Learning Perspective.
4. Farrar C. R., Worden K. (2012) Damage-Sensitive Features. In: Structural Health Monitoring: A Machine Learning Perspective. pp 161–243
5. Marafini F, Zini G, Barontini A, et al (2023) A proposal of classification for machine-learning vibration-based damage identification methods
6. Zini G, Betti M, Bartoli G (2022) A quality-based automated procedure for operational modal analysis. Mech Syst Signal Process 164:
7. TNO DIANA BV (2022) DIANA FEA, DIANA Finite Element Analysis Software, version 10.5.
8. Seif M, Main J, Weigand J, et al (2016) Temperature-Dependent Material Modeling for Structural Steels: Formulation and Application. Gaithersburg, MD
9. Aggarwal CC, (2017) One-Class Support Vector Machines . In: Outlier Analysis, pp 88-95
10. Servizio Idrologico Regionale (SIR) (2018) Archivio Dati Settore Idrologico e Geologico Regionale, Regione Toscana
11. Sokolova M, Lapalme G (2009) A systematic analysis of performance measures for classification tasks. Inf Process Manag 45:427–437